Design of a predictive semiactive suspension system

ALESSANRO GIUA, MAURO MELAS,
CARLA SEATZU AND GIAMPAOLO USAI

SUMMARY

In this paper we present an original design procedure for semiactive suspension systems. Firstly, we consider a target active control law that takes the form of a feedback control law. Secondly, we approximate the target law by controlling the damper coefficient f of the semiactive suspension. In particular, we examine two different kinds of shock absorbers: the first one uses magneto-rheological fluid instead of oil, while the second one is a solenoid valve damper. In both cases the nonlinear characteristics force-velocity of the damper are used to approximate the target law. To improve the efficiency of the proposed system, we take into account the updating frequency of the coefficient f and compute the expected value of f using a predictive procedure. We also address the problem of designing an asymptotic state observer that can be used not only to estimate the current state but also to predict the value that the state will take at the next sampling time.

Keywords: semiactive suspension, magneto-rheological damper, solenoid valve damper, linear quadratic regulator, H_2 norm.

1. INTRODUCTION

In this paper we deal with the problem of designing a control law for semiactive suspension systems.

A semiactive suspension [6, 7, 9, 13] consists of a spring and a damper but, unlike a passive suspension, the value of the damper coefficient f can be controlled and updated. In some types of suspensions, but this case is not considered here, it may also be possible to control the elastic constant λ_s of the spring. A semiactive suspension is a valid engineering solution — when it can reasonably approximate the performance of the active control — because it requires a low power controller that can be easily realized at a lower cost than that of a fully active one [3, 8]. Note, however, that a semiactive system clearly lacks other important secondary advantages of the fully

[1]Address correspondance to: A. Giua, M. Melas, C. Seatzu, G. Usai, Department of Electrical and Electronic Engineering, University of Cagliari, Piazza D'Armi, 09123, Cagliari, Italy.

This paper has been published as:
A. Giua, M. Melas, C. Seatzu, G. Usai, "Design of a predictive semiactive suspension system," *Vehicle System Dynamics*, Vol. 41, No. 4, pp. 277–300, Apr 2004.

active one, namely the ability to resist downward static forces due to passenger and baggage loads and to control the altitude of the vehicle.

Usually, the design of a semiactive suspension consists of two phases.

- First phase: choose a good active law, $u(\cdot)$ to be considered as a "target".
  The optimal control technique known as LQR [12] is probably the simplest way to design an active law for suspension systems and such an idea has been initially proposed by Thompson [16]. It takes the form of a state feedback law with constant gains, i.e., $u(t) = -\boldsymbol{K}\boldsymbol{x}(t)$, where $\boldsymbol{x}(t)$ is the state of the system.
- Second phase: choose at time t a suitable value of the damper coefficient $f(t)$ so that the force $u_s(\cdot)$ generated by the suspension system approximates as close as possible the target law $u(\cdot)$.
  If a linear model of the suspension is used, the force generated by the suspension system can be written as $u_s(t) = -\left[\lambda_s \;\; f(t) \;\; 0 \;\; -f(t)\right] \boldsymbol{x}(t)$, and the problem consists in choosing the value of $f(t)$ that minimizes the difference $|u(t) - u_s(t)|$

The main focus of some previous work [6] we did on this topic, was that of improving the first phase deriving better approaches for the design of a target control law. In particular, in [6] we used a technique called Optimal Gain Switching (OGS), originally proposed by Yoshida [17]. The OGS controller leads to better performances with respect to the LQR controller: in fact, while the latter uses a constant gain that realizes a particular trade-off between performance and comfort, the former adapts the trade-off to different road conditions and car velocities, applying different gains depending on the magnitude of the disturbance.

In this paper we complete our work focusing on the second phase (while in the first phase, for sake of simplicity, we use the standard LQR technique). In fact, we discuss three important engineering issues related to the control of the damper coefficient.

Non-linear behavior of the damper

The first contribution consists in taking into account the non-linear model of the damper (and of the spring) to generate a control force as close as possible to the target one. In particular we consider two different kinds of commercial dampers.

- The first one is a commercial damper [2] that uses magneto-rheological (MR) fluid instead of oil. The magneto-rheological response of MR fluids results from the polarization induced in suspended particles by the application of an external field. This system presents several advantages with respect to more conventional systems: it has no moving parts other than the piston and the rod itself; the required power is very low, and the response time is very fast. On the other hand, this technology is still new and presents some other shortcomings, such as hysteretic phe-

nomena (in-use thickening) and the impossibility of having small values of f, as discussed in the paper.

- The second one is a solenoid valve (SV) damper described in [15]. The value of the coefficient f is updated by appropriately varying the opening section where the oil flows from one chamber to the other one within the body damper. The main feature of the SV damper is the electro-valve where the variation of the opening section is realized thanks to the movement of a small cylinder along its own axis. The movement of the cylinder is governed by a magnetic field induced by an external current. This damper has a high response time but it is robust and reliable.

In both cases, the nonlinear behavior of the damper can be described through a family of nonlinear characteristics force-velocity: they are parameterized by constant current values in the MR case, and by constant values of the opening section in the SV case.

Response time of the controller and actuators

The second contribution consists in improving the performance of the resulting suspension system taking into account the delay time Δt that elapses between two updates of the damper coefficient.

First of all, it is important to observe that the on-board implementation of the controller is typically done using a microprocessor with a scan time Δt of the order of a few milliseconds. Every Δt time units the controller should choose — on the basis of the current value of the suspension velocity — the new damper coefficient f selecting a nonlinear characteristics force-velocity of the damper, so as to minimize the quadratic difference among the semiactive and the target control.

Furthermore, it is also necessary to take into account the physical limits on the updating frequency of the damper coefficient f. In fact, the actuators used to control the damper coefficient have a response time that cannot be neglected because it is usually larger than the scan time of the controller.

Depending on the response time of the actuators, two different approaches may be envisaged.

1. In the first approach we consider a scan time Δt comparable with the response time of the actuator. This means that if at time t the controller selects a value of f, i.e., a nonlinear characteristic, the damper will be able to switch to that characteristic only at time $t + \Delta t$.
   The new value of f at the generic time instant t is selected so as to minimize the quadratic difference $|u(t + \Delta t) - u_s(t + \Delta t)|$. In such a way, as proved via various numerical simulations, we are able to compensate the delay on the updating of f, thus producing a significant improvement on the system behavior [11].
   This approach is called *Unconstrained Update Control* (UUC) because at each step

we may freely choose to update to any other nonlinear characteristic.

2. In the second approach we consider a scan time Δt of the controller significantly smaller than the response time of the damper actuator. This means that if at time t the damper is working along a particular nonlinear characteristic, at time $t + \Delta t$ it cannot switch to an arbitrary one, but only to those "close enough" to the original one. In particular we consider the possibility of switching from a characteristic only to the one immediately over or under it.
   This means that when minimizing the quadratic difference $|u(t + \Delta t) - u_s(t + \Delta t)|$ an additional constraint is given from the fact that we may only move to an adjacent nonlinear characteristic. This approach is called *Incremental Update Control* (IUC).

The choice of the first or of the second approach depends on the particular damper technology.

As an example, in the case of the MR damper the updating frequency of f may take very high values, of the order of 250 Hz: for this suspension we only consider the first approach taking $\Delta t = 4$ ms [2].

On the contrary, in the case of the SV damper the updating frequency of f is much smaller, thus we apply both approaches. More precisely, we first consider a scan time $\Delta t = 30$ ms that is large enough to allow the system to switch to any nonlinear characteristics [15]. Finally, we consider a significantly smaller value of $\Delta t = 7$ ms such that the system may only switch to an adjacent nonlinear characteristic.

Observer predictor design

A control procedure that takes into account the delay time required to update the damper coefficient is viable only if we can make a good prediction on the value of the state $\boldsymbol{x}(t + \Delta t)$.

Note that in a suspension system the state is not directly accessible because measuring it is too expensive. Thus, an asymptotic state observer needs to be used. We show that the same observer can be used to predict the state at a future instant of time.

In particular we propose an original procedure for the design of an asymptotic state observer that well fits with the present application: the observer gain matrix is computed so as to minimize the H_2 norm of the transfer function matrix between the estimate error and the external disturbance. The results of various numerical simulations show that such an observer provides a good estimate of the system state $\boldsymbol{x}(t)$ and of its derivative, and thus can also be used to compute a reliable prediction of the systems state $\boldsymbol{x}(t + \Delta t)$.

Different simulations have been carried out, considering the effect of input disturbances caused by the road profile and the effect of non–null initial conditions on the state. The results of these simulations show that the semiactive suspension performs

reasonably well, and is a good approximation of the target active suspension, while it introduces significant improvements with respect to a completely passive suspension.

The paper is structured as follows. In the next section we present the dynamical model of the suspension dampers. In Section 3 we describe in detail the MR and the SV system In Section 4 we describe the procedure proposed for the observer design. The semiactive suspension design is the object of Section 5. The results of various numerical simulations are finally presented in Section 6.

2. DYNAMICAL MODEL OF THE SUSPENSION SYSTEM

Let us now consider the completely active suspension system with two degrees of freedom schematized in Figure 1.a. We used the following notation:

— M_1 is the equivalent unsprung mass consisting of the wheel and its moving parts;
— M_2 is the sprung mass, i.e., the part of the whole body mass and the load mass pertaining to only one wheel;
— λ_t is the elastic constant of the tire, whose damping characteristics have been neglected. Note that this is in line with almost all researchers who have investigated synthesis of active suspensions for motor vehicles as the tire damping is minimal;
— $x_1(t)$ is the deformation of the suspension with respect to (wrt) the static equilibrium configuration, taken as positive when elongating;
— $x_2(t)$ is the vertical absolute velocity of the sprung mass M_2;
— $x_3(t)$ is the deformation of the tire wrt the static equilibrium configuration, taken as positive when elongating;
— $x_4(t)$ is the vertical absolute velocity of the unsprung mass M_1;
— $u(t)$ is the control force produced by the actuator;
— $w(t)$ is the function representing the disturbance. It coincides with the absolute vertical velocity of the point of contact of the tire with the road.

It is readily shown that the state variable mathematical model of the system under study is given by [3]

$$\dot{\boldsymbol{x}}(t) = \boldsymbol{A}\boldsymbol{x}(t) + \boldsymbol{B}u(t) + \boldsymbol{L}w(t) \tag{1}$$

where $\boldsymbol{x}(t) = [x_1(t),\ x_2(t),\ x_3(t),\ x_4(t)]^T$ is the state, and where the constant matrices $\boldsymbol{A}$, $\boldsymbol{B}$ and $\boldsymbol{L}$ have the following structure:

$$\boldsymbol{A} = \begin{bmatrix} 0 & 1 & 0 & -1 \\ 0 & 0 & 0 & 0 \\ 0 & 0 & 0 & 1 \\ 0 & 0 & -\lambda_t/M_1 & 0 \end{bmatrix}, \qquad \boldsymbol{B} = \begin{bmatrix} 0 \\ 1/M_2 \\ 0 \\ -1/M_1 \end{bmatrix}, \qquad \boldsymbol{L} = \begin{bmatrix} 0 \\ 0 \\ -1 \\ 0 \end{bmatrix}.$$

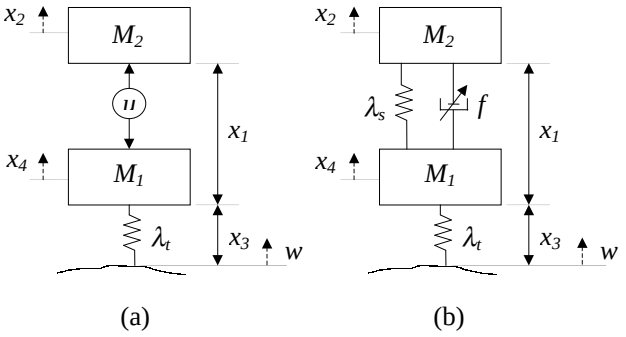

Fig. 1. Scheme of two degree-of-freedom suspension: (a) active suspension; (b) semiactive suspension.

Now, let us consider Figure 1.b that represents a conventional semiactive suspension composed of a spring, whose characteristics force-deformation is nonlinear, and a damper with adaptive characteristic coefficient $f = f(t)$.

The effect of this suspension is equivalent to that of a control force

$$u_s(t) = -\left[\, \lambda_s \;\; f(t) \;\; 0 \;\; -f(t) \,\right] \boldsymbol{x}(t). \tag{2}$$

Note that, as f may vary, $u_s(t)$ is both a function of $f(t)$ and of $\boldsymbol{x}(t)$. It is immediate to verify that the state variable mathematical model of the semiactive suspension is still given by equation (1) where $u(t)$ is replaced by $u_s(t)$.

3. THE MAGNETO-RHEOLOGICAL AND THE SOLENOID VALVE DAMPER

In this section we present in detail the main physical characteristics of both the magneto-rheological and the solenoid valve damper.

3.1. The magneto-rheological damper

The magneto-rheological damper is a shock absorber that uses Magneto-Rheological (MR) fluid instead of oil. In particular, we refer to a real existing damper shown in Figure 2.a, the *CARRERA*^{TM} *MagnetoShock*^{TM}, whose physical characteristics are given in [2].

The MR fluid is basically composed of micron sized particles of iron suspended in an oil base. The magneto-rheological response of MR fluids results from the polarization induced in suspended particles by the application of an external field. The interaction between the resulting induced bipoles causes the particles to form colum-

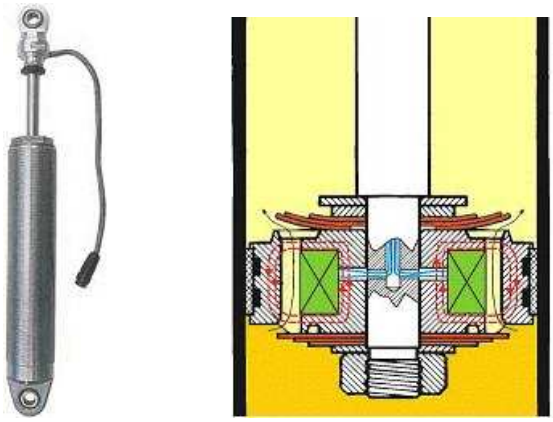

(a) (b)

Fig. 2. The *CARRERA*^{TM} *MagnetoShock*^{TM} and a scheme of its internal structure.

nar structures, parallel to the applied field. These chain-like structures restrict the motion of the fluid, thereby increasing the viscous characteristics of the suspension. The mechanical energy needed to yield the microstructure increases as the applied field increases resulting in a field dependent yield stress. In the absence of an applied field, MR fluids exhibit Newtonian-like behaviour [10].

The internal structure of the damper is sketched in Figure 2.b. The piston contains an annular orifice, through which the MR fluid passes, and an electromagnet. The controller varies the magnetic field of the electromagnet and the damping force varies proportionally. The MagnetoShock^{TM} has no moving parts (like valves, spring, etc.) other than the piston and rod itself.

The power required is very low (on the average, 3 W per shock) and the reaction time is very fast, usually less than 2 milliseconds. In its simplest form the damping force of the shock can be easily adjusted. It is capable of updating the damping force 500 times/second to each shock.

Figure 3 shows the nonlinear (static) characteristics force-velocity of the considered damper at different constant current values (in this figure, following a usual convention, a positive force corresponds to a positive velocity of deformation).

On the basis of the simulation results discussed in Section 6, the main drawback of this damper is not due to the updating frequency (that does not pose in practice any limitation) but lies in the fact that even with a null magnetic field the damper coefficient is too high. To improve the damper performance it should be necessary to

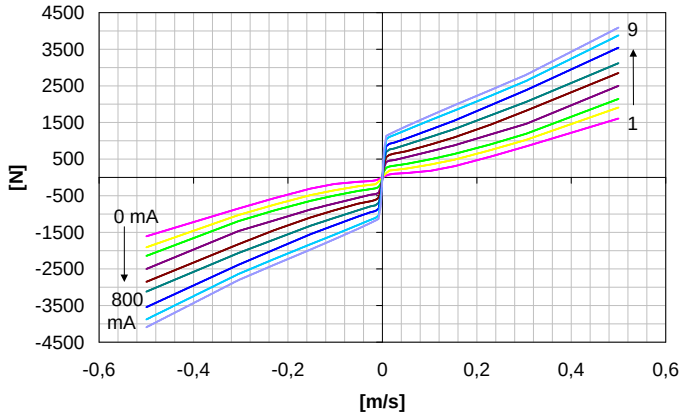

Fig. 3. The nonlinear characteristics of the MR damper.

have characteristic curves closer to the x axis than the one labeled "1" in Figure 3.

3.2. The solenoid valve damper

The main feature of the solenoid valve damper, frequently used in suspension systems of heavy vehicles, is the structure of the valves regulating the damping coefficient. These valves should be extremely rapid and precise, and at the same time should be capable of taking the stress due to the high values of the pressure within the damper.

The hydraulic circuit of the SV damper presented in [9] is sketched in Figure 4.a. A high speed electro-valve P_{v1} controls the pressure drop through the circuit, thereby appropriately updating the damping coefficient. A reservoir accomodates the oil displaced by the volume of the piston rod in the high pressure circuit and is pressurised with nitrogen gas (at a pressure P_{stat}) to prevent cavitation occurring. Note that the flow of oil always occur in the same direction, thus allowing to keep the structure of the system simple and compact. Moreover, the presence of the check valve and of the electro-valve at the opposite sides of the hydraulic circuit creates a physical separation among the low pressure circuit and the high pressure circuit.

A cross section view of the semiactive damper is shown in Figure 4.b where for simplicity the reservoir, the filter and the check valve are not shown. It is possible to distinguish three main parts that constitute the electro-valve: the hydraulic part, the electrical part and the position transducer. In the hydraulic part of the valve it occurs the variation of the cross section that allows to update the actual value of the damping coefficient. This updating can be realized thanks to a small cylinder that translates in

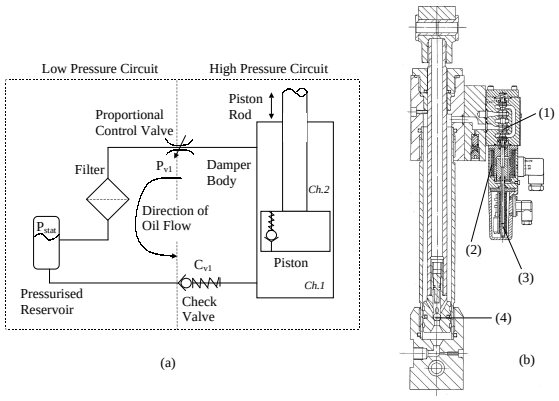

Fig. 4. (a) The hydraulic circuit of the semiactive damper. (b) A cross-section of the semiactive damper (reservoir, filter and check valve are not shown) where (1) is the spool, (2) is the solenoid, (3) is the position transducer and (4) is the piston check valve.

the direction of its own axis. The electrical part is basically constituted by a solenoid that can modify the position of the cylinder by simply applying an axial force. Finally, the position transducer is particularly useful when the damping coefficient requires to be updated at a very high frequency. Note that the feedback control of the cylinder position is also necessary due to the disturbance on the cylinder produced by the flow of oil in the hydraulic part of the valve.

Summarizing, such a suspension system requires two different control devices [9]. The first one is used to determine the position of the cylinder on the base of the difference among the target force and the actual force produced by the damper. Finally, the goal of the second control device is that of modifying the intensity of the current though the solenoid so as to reduce the difference among the required and the actual position of the cylinder.

In this paper we refer to a real existing SV damper whose physical (static) characteristics force-velocity are reported in Figure 5 and have been taken from [15]. However, in [15] the scaling of the axes is missing: we reconstruct it making reasonable assumptions. Each curve is parametrized by the position of the cylinder and consequently by the value of the opening section where the oil flows from one chamber to the other one within the damper body.

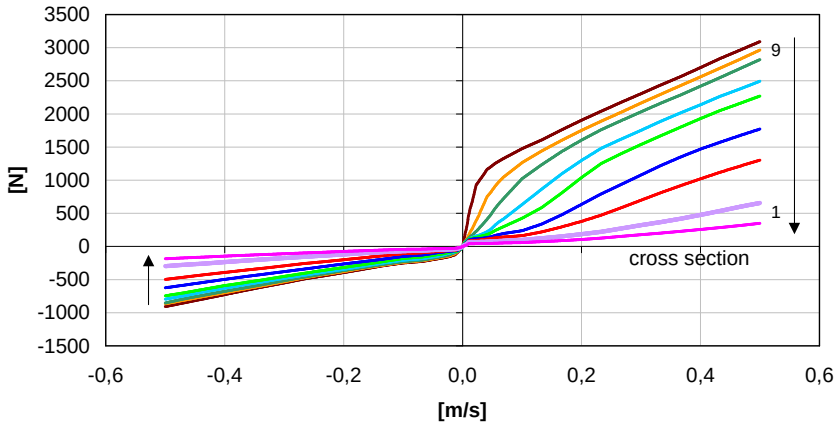

Fig. 5. The nonlinear characteristics of the SV damper.

4. OBSERVER DESIGN VIA H_2 NORM MINIMIZATION

The control law we will design in the following section requires the knowledge of the system state $\boldsymbol{x}$. Since not every component of $\boldsymbol{x}$ is directly measured, we construct an appropriate state observer. To do this, we choose a suitable matrix $\boldsymbol{C}$ for the output equation

$$\boldsymbol{y}(t) = \boldsymbol{C}\boldsymbol{x}(t). \tag{3}$$

If we assume

$$\boldsymbol{C} = \begin{bmatrix} 1\,0\,0\,0 \\ 0\,0\,1\,0 \end{bmatrix} \tag{4}$$

which corresponds to measuring the suspension and the tire deformation, the observability of the pair $(\boldsymbol{A}, \boldsymbol{C})$ is ensured.

The asymptotic state observer we propose has the structure of a Luenberger observer, i.e., it takes the form

$$\dot{\hat{\boldsymbol{x}}}(t) = \boldsymbol{A}\hat{\boldsymbol{x}}(t) + \boldsymbol{B}u(t) + \boldsymbol{K}_0(\boldsymbol{y}(t) - \hat{\boldsymbol{y}}(t)) \tag{5}$$

where $\hat{\boldsymbol{x}}(t)$ is the state estimate and $\hat{\boldsymbol{y}}(t) = \boldsymbol{C}\hat{\boldsymbol{x}}(t)$.

$\boldsymbol{K}_0$ is the gain matrix that has to be determined so as to impose the desired error dynamics:

$$\dot{\boldsymbol{e}}(t) = (\boldsymbol{A} - \boldsymbol{K}_0\boldsymbol{C})\boldsymbol{e}(t) + \boldsymbol{L}w(t). \tag{6}$$

The gain matrix $\boldsymbol{K}_0$ may be chosen so as to impose a given set of eigenvalues to $(\boldsymbol{A} - \boldsymbol{K}_0\boldsymbol{C})$. Nevertheless, in the presence of external disturbances, as in the case at hand, this does not ensure a satisfactory behaviour. This motivates the non–standard procedure used in this paper for the design of the state observer, that is described in detail in the following.

Firstly, let us observe that we can always assume that the initial estimation error is null, i.e., $\boldsymbol{e}(0) = \boldsymbol{0}$, being x_1 and x_3 measurable variables and x_2 and x_4 vertical velocities that are null at the very first time instant of evolution, when the car is motionless.

By virtue of this consideration, the Laplace–transform of the above equation (6) takes the form

$$\boldsymbol{E}(s) = [s\boldsymbol{I} - (\boldsymbol{A} - \boldsymbol{K}_0\boldsymbol{C})]^{-1}\boldsymbol{L}W(s) \tag{7}$$

where $\boldsymbol{I}$ is the fourth order identity matrix, and $\boldsymbol{E}(s)$ and $W(s)$ are the Laplace–transformation of $\boldsymbol{e}(t)$ and $w(t)$, respectively.

Now, we determine the observer matrix $\boldsymbol{K}_0$ by simply minimizing the H_2 norm [1] of the transfer function matrix between the estimate error and the external disturbance, i.e.,

$$\boldsymbol{F}(s) = [s\boldsymbol{I} - (\boldsymbol{A} - \boldsymbol{K}_0\boldsymbol{C})]^{-1}\boldsymbol{L}.$$

In such a way we can be sure that we are minimizing the effect of the disturbance on the error estimate. In fact, the minimization of the H_2 norm of the above transfer function $\boldsymbol{F}(s)$ leads to the minimization of $\|e(t)\|_2^2$ for any external input of the form $w(t) = w_0\delta(t)$ [4]. Moreover, as formally proved in [4], the minimization of the H_2 norm of a transfer function is equivalent to the minimization of the RMSV of the output (in such a case the estimate error) when the input is a white noise signal.

5. SEMIACTIVE SUSPENSION DESIGN

In this section we first discuss how the target active control law has been determined. Then we show how such a control law, that requires an actuator, may be approximated by a semiactive suspension, whose varying parameter is the characteristic coefficient of the damper f.

[1] Let $\boldsymbol{G}(s) : \mathbb{C} \to \mathbb{R}^{m\times n}$ be a transfer function matrix. The H_2 norm of $\boldsymbol{G}$ is:

$$\| \boldsymbol{G} \|_2 = \left(\frac{1}{2\pi} \int_{-\infty}^{\infty} trace\{\boldsymbol{G}^H(j\omega)\boldsymbol{G}(j\omega)\} d\omega \right)^{1/2},$$

where ^{H} denotes complex conjugate transposition.

5.1. Target active control law

The design of the active suspension requires determining a suitable control law $u(\cdot)$ for system (1). To this end, we first determine the control law $u(\cdot)$ that minimizes a performance index of the form

$$J = \int_0^\infty (\boldsymbol{x}^T(t)\boldsymbol{Q}\boldsymbol{x}(t) + ru^2(t))dt \tag{8}$$

where $\boldsymbol{Q}$ is positive semidefinite and $r > 0$. As well known from the literature [12], the solution of this problem can be easily computed by simply solving an algebraic Riccati equation, and takes the form of a feedback control law:

$$u(t) = -\boldsymbol{K}\boldsymbol{x}(t). \tag{9}$$

Obviously, when the system state is not directly measured, but is reconstructed via an asymptotic observer, the above control law is replaced by

$$u(t) = -\boldsymbol{K}\hat{\boldsymbol{x}}(t) \tag{10}$$

where $\hat{\boldsymbol{x}}(t)$ is the state estimate.

5.2. Semiactive approximation

In this subsection we show how the active target control law u given by (10) may be approximated using a semiactive suspension, taking into account the nonlinear characteristics force-velocity of the damper (see Figures 3 and 5). The aim of the controller is that of selecting the nonlinear characteristic that minimizes the difference among the resulting semiactive control force and the target active control force. The nonlinear characteristic force-deformation of the spring is also taken into account.

Note that a certain time Δt, depending on the physical system, is necessary to update the damper coefficient. In several previous works the delay time Δt has been neglected. This implies that, if at the generic time instant t we select a certain characteristic, then such a characteristic will only be reached at the time instant $t + \Delta t$.

To overcome such a problem, in this paper our goal at time t becomes that of minimizing the quadratic difference among the semiactive control force and the target active control force at the time instant $t + \Delta t$, namely

$$|u(t + \Delta t) - u_s(t + \Delta t)|.$$

The target control force at time $t + \Delta t$ from (10) should be equal to

$$u(t + \Delta t) = -\boldsymbol{K}\hat{\boldsymbol{x}}(t + \Delta t).$$

The semiactive control force at time $t + \Delta t$ may be written as:

$$\begin{aligned} u_s(t+\Delta t) &= -\lambda_s(x_1(t+\Delta t)) \cdot x_1(t+\Delta t) - f(t+\Delta t) \cdot (x_2(t+\Delta t) - x_4(t+\Delta t)) \\ &\simeq -\lambda_s(\hat{x}_1(t+\Delta t)) \cdot \hat{x}_1(t+\Delta t) - F_d(t+\Delta t) \end{aligned}$$

where $\hat{x}_i$ denotes the estimate of state x_i generated by the observer, thus

$$-\lambda_s(\hat{x}_1(t+\Delta t)) \cdot \hat{x}_1(t+\Delta t)$$

denotes the force due to the spring at time $t + \Delta t$; while

$$F_d(t+\Delta t) = f(t+\Delta t) \cdot (\hat{x}_2(t+\Delta t) - \hat{x}_4(t+\Delta t))$$

is the force due to the damper at the time instant $t + \Delta t$.

Therefore, given the nonlinear characteristics of the damper, we restrict our attention to only those values of the force that can be generated when the suspension velocity deformation is equal to $\hat{x}_2(t+\Delta t) - \hat{x}_4(t+\Delta t) \simeq \dot{x}_1(t+\Delta t)$. We select the characteristic that generates the force that minimizes the quadratic difference:

$$|-\boldsymbol{K}\hat{\boldsymbol{x}}(t+\Delta t) + \lambda_s(\hat{x}_1(t+\Delta t)) \cdot \hat{x}_1(t+\Delta t) + F_d(t+\Delta t)|$$

and we denote it $F_d^*(t+\Delta t)$.

At this point we can follow two different procedures, depending on the value of Δt, and consequently on the considered damper.

Assume that the delay time Δt is large enough to ensure that within the time interval $[t, t+\Delta t]$ we can move from any nonlinear characteristic to any other one. As an example, this is the case when the semiactive suspension uses a MR damper and the delay time of the controller is equal to $\Delta t = 4$ ms [2]. The procedure we adopt may be briefly be summarized as follows.

Procedure 5.1 (UUC: Unconstrained Updating Control)**.** At time t we select the nonlinear characteristic that at time $t + \Delta t$ will provide the force $F_d^*(t+\Delta t)$. ■

The same procedure may also be adopted when using the solenoid valve damper. However, in this case, the updating frequency of the coefficient f is significantly smaller than in the MR case and the UUC procedure may be applied provided that the value of the delay time of the controller is taken equal to $\Delta t = 30$ ms [9].

On the contrary, when the updating time Δt of the controller is not large enough to enable us to arbitrarily move among the nonlinear characteristics, the above procedure cannot be no longer adopted. In the case that Δt only enables us to switch among adjacent characteristics, we suggest to use the following procedure.

Procedure 5.2 (IUC: Incremental Updating Control)**.** At time t we select the adjacent nonlinear characteristic that at time $t + \Delta t$ will provide a force as close as possible

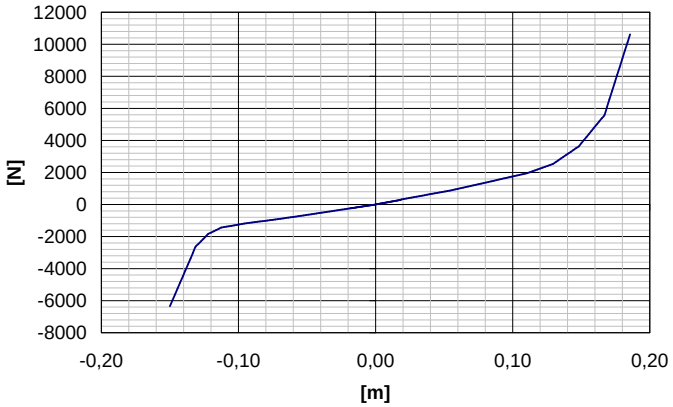

Fig. 6. The nonlinear characteristic of the suspension spring.

to $F_d^*(t+\Delta t)$. In particular, given the actual value of the force $u(t)$ at time t, three different cases may occur:

- if $u(t) < F_d^*(t+\Delta t)$ we switch to the adjacent superior characteristic;
- if $u(t) = F_d^*(t+\Delta t)$ we keep the actual characteristic unaltered;
- if $u(t) > F_d^*(t+\Delta t)$ we switch to the adjacent inferior characteristic.

■

This procedure has been adopted in the case of the SV damper when the controller has an updating delay that is equal to $\Delta t = 7$ ms.

6. APPLICATION EXAMPLE

In this section we discuss in detail the results of several simulations. First, however, we explain the choices we have made for the various parameters.

The proposed procedure has been applied to the quarter car suspension shown in Figure 1, with values of the parameters taken from [16]: $M_1 = 28.58$Kg, $M_2 = 288.90$Kg, $\lambda_t = 155900$N/m. In the simulation we used the nonlinear characteristic of the suspension spring given in Figure 6. Finally, the characteristics of the dampers are those shown in Figures 3 and 5, respectively.

The matrices $\boldsymbol{Q}$ and r of the performance index J have been taken from [16] and

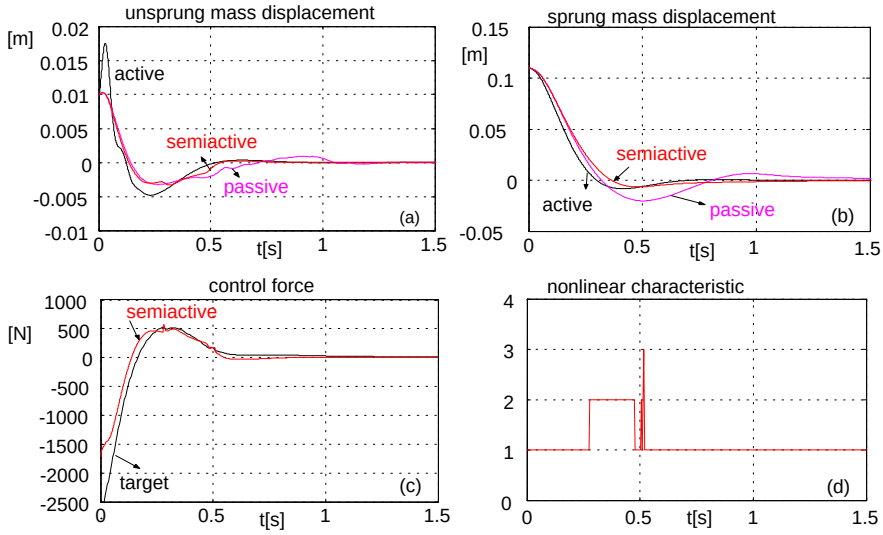

Fig. 7. The results of simulation 1 when the semiactive suspension uses a MR damper.

are the same as those already used in [4, 6]:

$$\boldsymbol{Q} = diag\{1, 0, 10, 0\},\ r = 0.8 \cdot 10^{-9}.$$

Thus, the resulting feedback control matrix is

$$\boldsymbol{K} = \begin{bmatrix} 35355 & 4827 & -21879 & -1386 \end{bmatrix}.$$

For the computation of the observer matrix we used the software tools available in Matlab: `fmins` is the minimization procedure and `normh2` computes the H_2 norm. We determined

$$\boldsymbol{K}_o = \begin{bmatrix} 176.1 & 1334.4 & 1.9 & -145.7 \\ 51.3 & 426.1 & 1852.5 & -5501.4 \end{bmatrix}^T.$$

To show the performance of the proposed semiactive suspension design, we have simulated two different situations.

6.1. Simulation 1

In the first simulation we consider an initial state different from zero and no external disturbance. In particular, we assume $\boldsymbol{x}(0) = \hat{\boldsymbol{x}}(0) = [0.1\ 0\ 0.01\ 0]^T$.

We first assume that the semiactive suspension uses a MR damper and we take $\Delta t = 4$ ms.

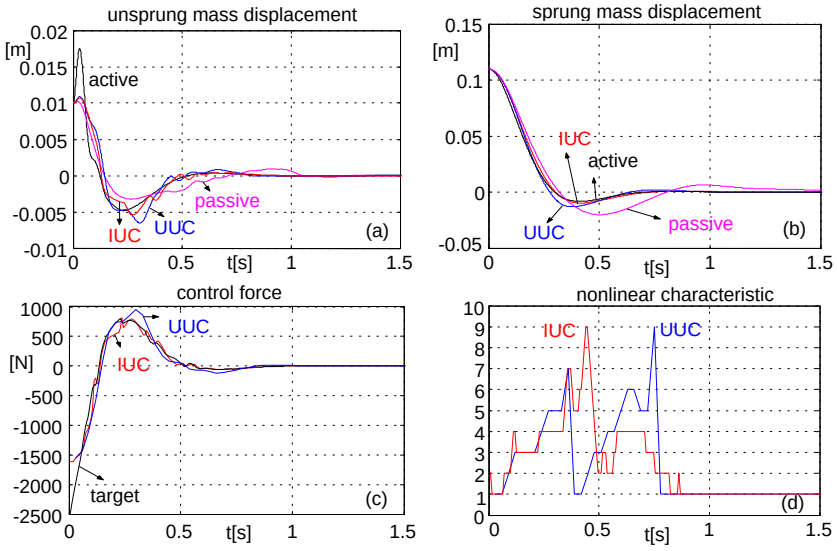

Fig. 8. The results of simulation 1 when the semiactive suspension uses a SV damper.

The results of this simulation are shown in Figure 7. In the upper part, plots (a)-(b) compare the unsprung and the sprung mass displacement of the semiactive suspension with that of a completely passive suspension and a purely active one. Note that the spring of the passive suspension is the same as that used in the semiactive suspension, while the nonlinear characteristic of the damper is that one denoted with the number 7 in Figure 3. In particular, looking at plot (b) that shows the most significant variable, we can conclude that the semiactive system guarantees better performance than the passive one [4]. In fact, in such a case the behaviour of the semiactive suspension system in terms of the sprung mass displacement, is quite similar to that obtained using the purely active system.

The lower left plot (c) compares the target force with the control force produced by the semiactive suspension.

Finally, plot (d) shows the values of the index denoting the current nonlinear characteristic during the evolution of the semiactive suspension.

Now, let us assume that the semiactive suspension uses a SV damper. The same simulation is carried out with both the UUC procedure and the IUC procedure. In the first case we assume $\Delta t = 30$ ms, while in the second case we assume $\Delta t = 7$ ms.

The results of this simulation are shown in Figure 8. The upper two plots (a)-(b) compare the unsprung and the sprung mass displacement of the semiactive suspension (using both the UUC and the IUC procedure) with that of a completely passive sus-

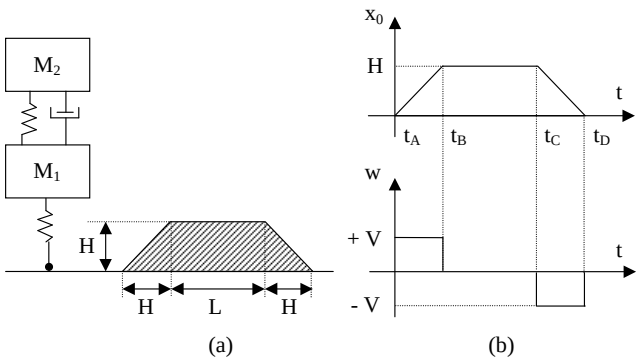

Fig. 9. Geometrical characteristics of the bump (a) and the resulting disturbance $w(t) = \dot{x}_0(t)$ (b).

pension and a purely active one. As we can note, both in the case of the UUC and in the case of the IUC approach, the semiactive system better approximate the active system than the passive one [4]. We may also conclude that the /IUC procedure provides a more satisfactory behaviour in terms of comfort with respect to the UUC procedure. In fact, in such a case the behaviour of the semiactive suspension system in terms of the sprung mass displacement, is practically the same as that obtained using the purely active system.

The lower left plot (c) compares the target force with the control force produced by the semiactive suspension, both in the case of the IUC and in the case of the UUC procedure. We can observer that in the case of the IUC procedure, the difference among the target active control force and the semiactive control force is quite negligible.

Finally, plot (d) shows the values of the index denoting the current nonlinear characteristic during the evolution of the semiactive suspension, both in the case of the UUC and in the case of the IUC procedure.

6.2. Simulation 2

In the second simulation we consider null initial conditions, i.e., $\boldsymbol{x}(0) = \hat{\boldsymbol{x}}(0) = \mathbf{0}$ and assume that an external disturbance is acting on the system, caused by a bump in the road profile. The geometrical characteristics of the bump are shown in Figure 9.a.

We make the hypothesis that the velocity of the vehicle keeps at a constant value V during all the time period of interest.

Moreover, we assume that the point of contact of the tire with the road perfectly follows the road profile, or equivalently we assume that no loss of contact between wheel and road may occur. Finally, we assume that the damping of the tire is negligible

and its dynamical behaviour may be modeled through a pure elastic constant.

Under these hypothesis the vertical position x_0 of the point of contact of the tire with the road depends not only on the shape of the bump, but also on the velocity V of the vehicle. The value of x_0 with respect to time t is shown in Figure 9.b where

$$(t_B - t_A) = (t_D - t_C) = H/V,$$

being the velocity of the vehicle equal to V during all the time period of interest.

As a consequence, the external disturbance $w(t)$, i.e., the vertical velocity of the point of contact of the tire with the road, varies with respect to time as shown in Figure 9.b.

The results of this simulation test are shown in Figures 10 and 11, where we have taken $H = 25$ mm, $L = 50$ mm, and $V = 10$ m/s. In particular, in Figure 10 are reported the results of that simulation that has been carried out assuming that the semiactive suspension uses a magneto-rheological damper, while in Figure 11 we have reported the results obtained assuming that the semiactive suspension uses a solenoid valve damper and the IUC procedure. Note that for brevity's requirement the graphical results relative to the UUC approach are omitted here [11]. Nevertheless a comparison among the two updating procedures in terms of performance index is reported in Table 1.

In the following we explain in detail the physical meaning of both Figures 10 and 11, where the same notation has been used.

Figure (a) shows the road profile x_0 (thin line) along with the unsprung mass displacement $x_3 + x_0$ (thick line). Figure (b) shows the road profile x_0 (thin line) along with the sprung mass displacement $x_1 + x_3 + x_0$ (thick line). It is possible to observe that the semiactive suspensions well behaves in front of the abrupt obstacle, smoothing the movement of the sprung mass.

Figure (c) compares the sprung mass displacement in the case of the semiactive suspension (thick line) and in the case of a completely passive suspension (thin line), while plot (d) compares the sprung mass displacement in the case of the semiactive suspension (thick line) and in the case of the target active suspension (thin line). As it can be noted, in both cases the behaviour of the semiactive suspension is intermediate between that of the passive and active suspension.

Figure (e) compares the target force (thin line) with the control force produced by the semiactive suspension (thick line). We can observe that in both cases the variation of f guarantees a satisfactory approximation.

Figure (f) shows the values of the index denoting the current nonlinear characteristic during the evolution of the semiactive suspension.

Figures (g) – (j) show the efficiency of the asymptotic state observer used during simulations. In plot (g) we have reported the evolution of the first state variable x_1, while in plot (h) we have reported the evolution of its error estimate $e_1 = x_1 - \hat{x}_1$. Figure (i) shows the evolution of $\dot{x}_1$, while $\dot{e}_1 = \dot{x}_1 - \dot{\hat{x}}_1$ is reported in plot (j). We

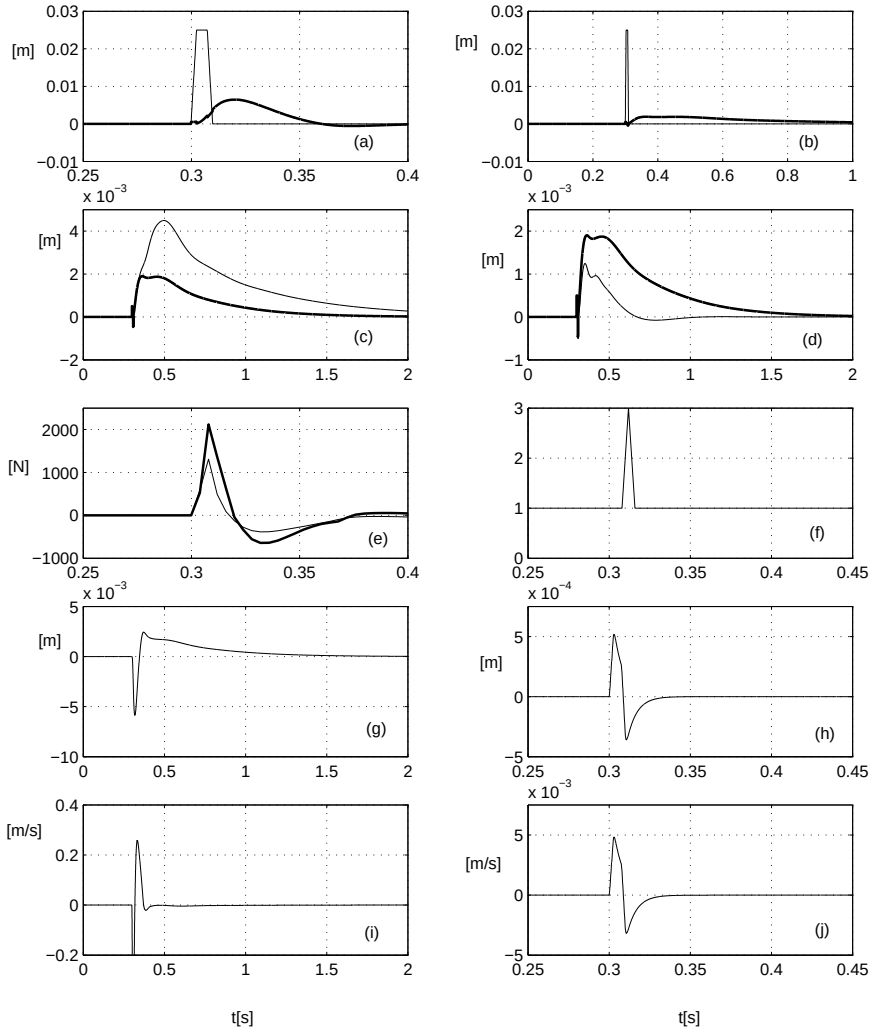

Fig. 10. The results of Simulation 2 when the semiactive suspension uses a MR damper.

can observe that it provides a good evaluation of both the state variables and their derivatives.

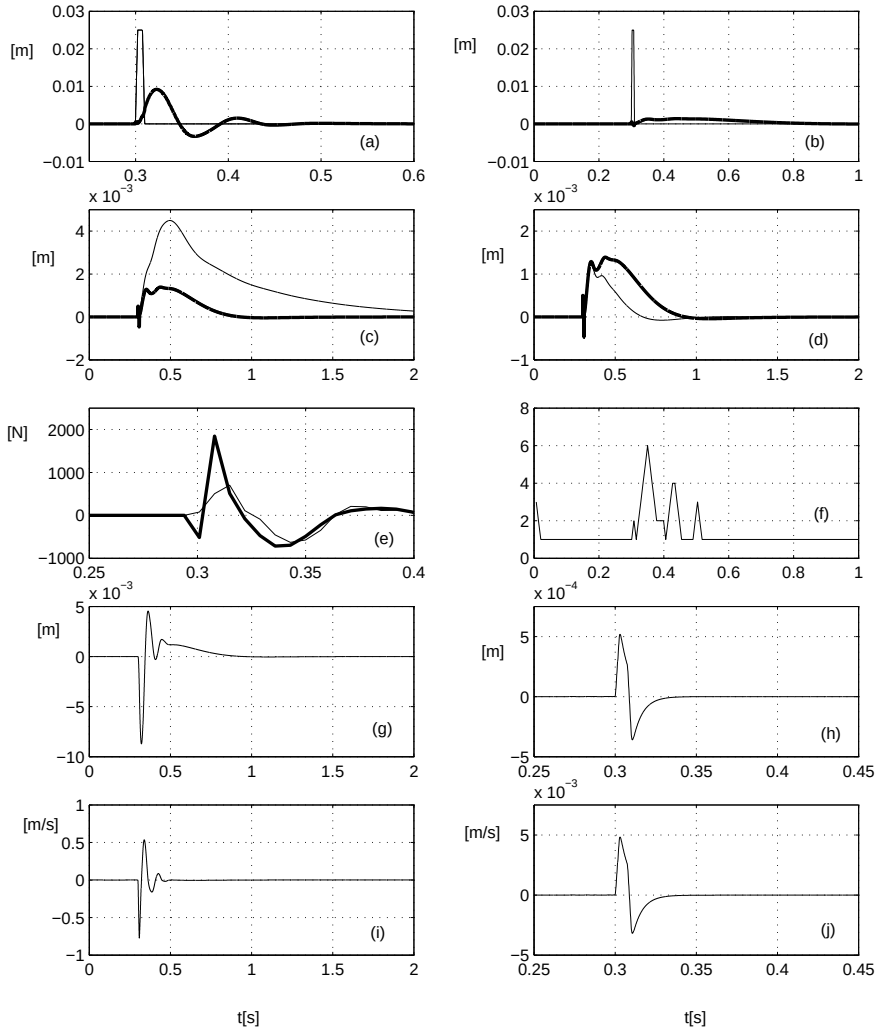

Fig. 11. The results of Simulation 2 when the semiactive suspension uses a SV damper and the IUC procedure.

6.3. Simulation 3

In the third simulation we assume that the disturbance $w(t)$ is caused by the uneven road profile and is assumed to be a white noise signal, which is equivalent to saying that the longitudinal road profile x_0 can be represented by an integrated white noise

[6, 8, 16]. Here, the road roughness characteristics are expressed by a signal whose PSD distribution function is [8]:

$$\Psi(\omega) = \frac{cV}{\omega^2 + \alpha^2 V^2} \tag{11}$$

where $c = (\sigma^2/\pi)\alpha$. Here σ^2 denotes the road roughness variance and V the vehicle speed, whereas the coefficients c and α depend on the type of road surface. The product is the power spectrum of the white noise. The signal $x_0(t)$, whose PSD is given by (11), may be obtained as the output of a linear filter expressed by the differential equation [3]

$$\dot{x}_0(t) = -\alpha V x_0(t) + w(t). \tag{12}$$

If we assume $\alpha^2 V^2 << \omega^2$, we have $\Psi(\omega) = cV/\omega^2$ and $\dot{x}_0(t) = w(t)$, i.e., the road profile is integrated white noise.

In particular, in the numerical simulation reported here, we have taken $\alpha = 0.15\text{m}^{-1}$ and $\sigma^2 = 9$ mm^2 that correspond to an asphalt road profile. Finally, we have assumed $V = 30$ m/s.

Figure 12 shows the results obtained when the semiactive suspension uses a SV damper and the IUC approach. For brevity's sake the results obtained in the other two cases are omitted here but have been reported in [11]. A numerical comparison among the three proposed solutions in terms of performance index is given in Table 1.

In particular, plot (a) shows the road profile x_0 (thin line) along with the unsprung mass displacement (thick line). Figure (b) shows the road profile (thin line) along with the sprung mass displacement (thick line). It is possible to observe that the semiactive suspension filters the high frequencies smoothing the movement of the sprung mass.

Figure (c) compares the sprung mass displacement in the case of the semiactive suspension (thick line) and in the case of a completely passive suspension (thin line). It is immediate to observe the significant improvements deriving from adapting f.

Figure (d) compares the sprung mass displacement in the case of the semiactive suspension (thick line) and in the case of the target active suspension. (thin line). As it can be noted, the semiactive suspension provides a good approximation of the active target system.

Figure (e) compares the target force (thin line) with the control force produced by the semiactive suspension (thick line). This plot shows how the selected nonlinear characteristic, or equivalently the selected value of f, guarantees a good approximation of the target control force. Note that, due to the small magnitude of the external disturbance considered here, the nonlinear characteristic always keeps the same during all the numerical simulation. In particular, it always keeps equal to the first one.

Figures (f)–(i) show the efficiency of the proposed observer. More precisely, in plot (f) we have reported the evolution of the first state variable x_1, while in plot (g) we have reported the evolution of its error estimate $e_1 = x_1 - \hat{x}_1$. Figure (h) shows the

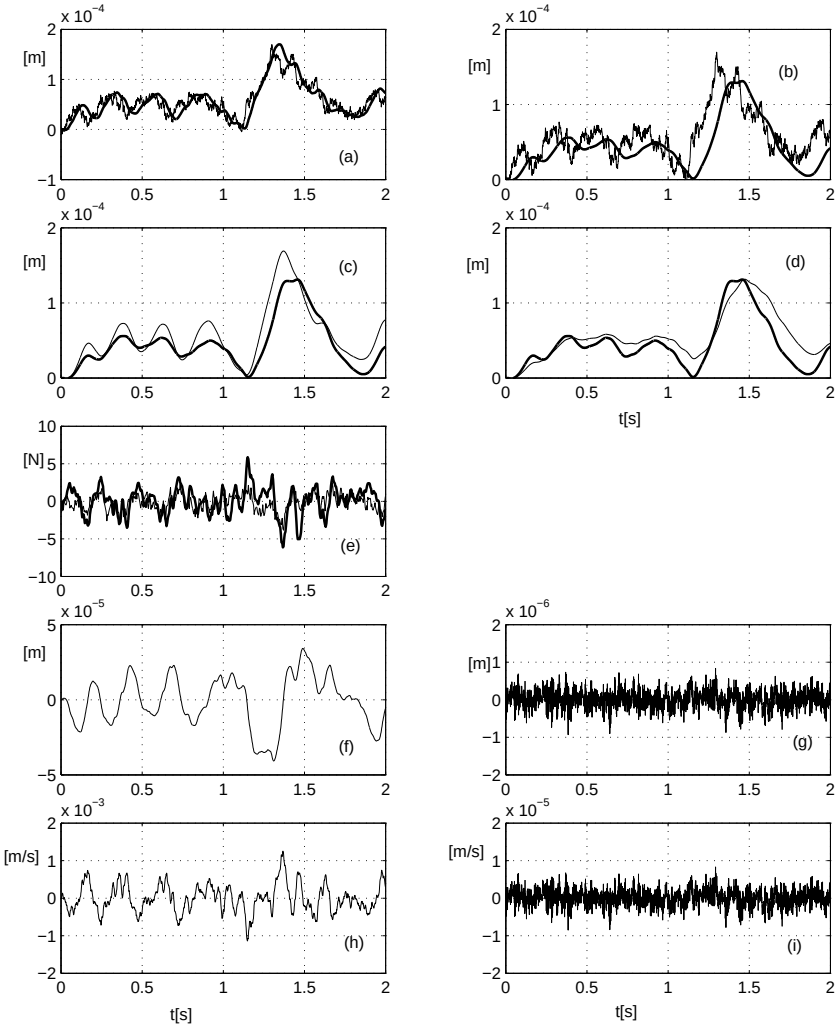

Fig. 12. The results of Simulation 3 when the semiactive suspension uses a SV damper and the IUC approach.

evolution of $\dot{x}_1$, while $\dot{x}_1 = \dot{x}_1 - \dot{\hat{x}}_1$ is reported in plot (i).

Similar results are obtained when the semiactive suspension uses either a MR damper or a SV damper and the UUC approach.

	passive	active	MR	SV (UUC)	SV (IUC)
Simulation 1	$1.736 \cdot 10^{-3}$	$1.606 \cdot 10^{-3}$	$1.688 \cdot 10^{-3}$	$1.675 \cdot 10^{-3}$	$1.652 \cdot 10^{-3}$
Simulation 2	$7.781 \cdot 10^{-5}$	$7.355 \cdot 10^{-5}$	$7.587 \cdot 10^{-5}$	$7.587 \cdot 10^{-5}$	$7.368 \cdot 10^{-5}$
Simulation 3	$1.952 \cdot 10^{-8}$	$8.915 \cdot 10^{-9}$	$1.4007 \cdot 10^{-8}$	$1.274 \cdot 10^{-8}$	$1.099 \cdot 10^{-8}$

Table 1. A comparison among the different semiactive suspensions.

6.4. A comparison among the different approaches

In this subsection we provide a brief comparison among the different kinds of semiactive suspension systems considered in this paper. Such a comparison is briefly summarized in Table 1 where we have reported the value of the performance index J corresponding to all the simulation test cases examined. Such an analysis enables us to conclude that in all cases examined the semiactive suspension system always provides a good approximation of the fully active suspension system, while producing significant improvements with respect to the purely passive suspension system. Finally, we may also conclude that the best results in terms of the performance index J are obtained when the semiactive suspension uses a SV damper and the IUC approach. This enables us to conclude that the updating frequency does not pose in practice a relevant limitation. The main drawback of the semiactive suspension systems examined lies in the fact that even the lowest obtainable values of the damper coefficient are often too high. Clearly this problem is much more pregnant in the case of the MR system, as it can be easily argued from its nonlinear characteristics. Thus, to improve the damper performance it is necessary to have characteristic curves closer to the x axis than the one labeled "1" in Figure 3.

7. CONCLUSIONS

In this paper we have presented a two–phase design technique for semiactive suspensions.

The first phase of the project requires the design of an asymptotic state observer that has been computed by minimizing the H_2 norm of the transfer function matrix among the error state estimate and the external disturbance. Then, the target active control law has been obtained by solving an LQR problem.

In the second phase, this target law is approximated by controlling the damper coefficient of the semiactive suspension. In particular, we have taken into account the delay time Δt required for the updating of f: we have assumed that the new value of f is chosen so as to minimize the difference between the target and the semiactive control law at the time instant $t + \Delta t$. In such a way we can be sure that when the computed value of f is really imposed, then the semiactive force is as close as possible

to the target one. Two different procedures have been suggested depending on the particular value of Δt and on the physical damper used in the suspension system.

The nonlinear behaviour of both the damper and the spring is also take into account to approximate the target active control law.

Several numerical simulations have been carried out considering a real existing SV damper and a MR damper.

REFERENCES

1. R. Caponetto, G. Fargione, A. Risitano, D. Tringali, "Soft computing for the design and optimization of a fuzzy Sky-Hook controller for semiactive suspensions," *XXX Convegno Nazionale AIAS* (Alghero, Italy), September 2001 (in Italian).
2. Carrera web site, http://www.carreraschocks.com, 2002.
3. G. Corriga, S. Sanna, G. Usai, "An optimal tandem active-passive suspension for road vehicles with minimum power consumption," *IEEE Trans. on Industrial Electronics*, Vol. 38, No. 3, pp. 210–216, 1991.
4. G. Corriga, A. Giua, G. Usai, "An H_2 formulation for the design of a passive vibration–isolation system for cars," *Vehicle System Dinamics*, Vol. 26, pp. 381–393, 1996.
5. M. Ebau, A. Giua, C. Seatzu, G.Usai, "Semiactive suspension design taking into account the actuator delay," *Proc. 40th IEEE Conference on Decision and Control* (Orlando, Florida), pp. 93–98, December 2001.
6. A. Giua, C. Seatzu, G. Usai, "Semiactive suspension design with an Optimal Gain Switching target," *Vehicle System Dinamics*, Vol. 31, pp. 213–232, 1999.
7. E. Göring, E.C. von Glasner, R. Povel, P. Schützner, "Intelligent suspension systems for commercial vehicles," *Proc. Int. Cong. MV2, Active Control in Mechanical Engineering* (Lyon, France), pp. 1–12, June 1993.
8. A. Hac, "Suspension optimization of a 2-DOF vehicle model using stochastic optimal control technique," *Journal of Sound and Vibration*, Vol. 100, N. 3, pp. 343–357, 1985.
9. K.J. Kitching, D.J. Cole, D. Cebon, "Performance of Semi-Active Damper for Heavy Vehicles," *ASME Journal of Dynamic Systems Measurement and Control*, Vol.122, pp.498-506, 2000.
10. Lord Corporation web site, http://www.lord.com, 2002.
11. M. Melas, "Nonlinear semiactive suspension design," *Laurea Thesis*, University of Cagliari, Italy, October 2002 (in Italian).
12. K. Ogata, *Modern control engineering*, Prentice Hall International Editions, 1990.
13. V. Roberti, B. Ouyahia, A. Devallet, "Oleopneumatic suspension with preview semi-active control law," *Proc. Int. Cong. MV2, Active Control in Mechanical Engineering* (Lyon, France), Vol. 1, June 1993.
14. D. Sammier, "Modeling and control of suspension systems for road vehicle," *Ph.D. Thesis*, Lab. of Automatic Control of Grenoble, France, November 2001 (in French).
15. D. Sammier, O. Sename, L. Dugard, "Commande par placement de poles de sospensions automobiles," *Conf. Int. Francophone d'Automatique*, (Nantes, France), July 2002 (in French).
16. A.G. Thompson, "An active suspension with optimal linear state feedback," *Vehicle System Dynamics*, Vol. 5, pp. 187–203, 1976.
17. K. Yoshida, Y. Nishimura, Y. Yonezawa, "Variable gain feedback for linear sampled-data systems with bounded control," *Control Theory and Advanced Technology*, Vol. 2, No. 2, pp. 313–323, June 1986.